SURFACE X-RAY SCATTERING MEASUREMENTS OF THE SUBSTRATE INDUCED SPATIAL MODULATION OF AN INCOMMENSURATE ADSORBED MONOLAYER

by

Michael F. Toncy*, Joseph G. Cordon*, Mahesh G. Samant*,
Gary L. Borges*, Owen R. Melroy*, Lung-Shan Kau*, David
G. Wiesler*, Dennis Yee and Larry B. Sorensen**

AD-A232 625

*IMB Research Division
Almaden Research Center
650 Harry Road
San José, California 95120-6099

**Department of Physics FM-15
University of Washington
Seattle, WA 98195

DTIC
ELECTE
MAR 0 1 1991
B

*This statement should also appear in Item 10 of Document Control Data
- DD Form 1473. Copies of form available from congnizant contract
administrator.

91 3   04 024

REPORT DOCUMENTATION PAGE

1a. REPORT SECURITY CLASSIFICATION	1b RESTRICTIVE MARKINGS

2a. SECURITY CLASSIFICATION AUTHORITY	3 DISTRIBUTION / AVAILABILITY OF REPORT
2b. DECLASSIFICATION / DOWNGRADING SCHEDULE	

4. PERFORMING ORGANIZATION REPORT NUMBER(S)	5 MONITORING ORGANIZATION REPORT NUMBER(S)
Technical Report #5	

6a. NAME OF PERFORMING ORGANIZATION	6b OFFICE SYMBOL (If applicable)	7a NAME OF MONITORING ORGANIZATION
Physics Department University of Puerto Rico		

6c. ADDRESS (City, State, and ZIP Code)	7b ADDRESS (City, State, and ZIP Code)
Río Piedras, P.R. 00931-3343	

8a. NAME OF FUNDING / SPONSORING ORGANIZATION Chemistry Office of Naval Research	8b. OFFICE SYMBOL (If applicable) Code 472	9 PROCUREMENT INSTRUMENT IDENTIFICATION NUMBER RCT Project 4133002---05

8c. ADDRESS (City, State, and ZIP Code)	10 SOURCE OF FUNDING NUMBERS			
Arlington Virginia 22217-5000	PROGRAM ELEMENT NO	PROJECT NO.	TASK NO	WORK UNIT ACCESSION NO

11. TITLE (Include Security Classification)
SURFACE X-RAY SCATTERING MEASUREMENTS OF THE SUBSTRATE INDUCED SPATIAL MODULATION OF AN INCOMMENSURATE ADSORBED MONOLAYER

12. PERSONAL AUTHOR(S) M.F. Toney, J.G. Gordon, M.G. Samant, G.L. Borges, O.R. Melroy, L.S. Kau, D.G. Wiesler, D. Yee and L.B. Sorensen.

13a. TYPE OF REPORT Summary	13b. TIME COVERED FROM _____ TO _____	14. DATE OF REPORT (Year, Month, Day) 1-29-91	15. PAGE COUNT 32

16. SUPPLEMENTARY NOTATION

17 COSATI CODES			18. SUBJECT TERMS (Continue on reverse if necessary and identify by block number)
FIELD	GROUP	SUB-GROUP	

19 ABSTRACT (Continue on reverse if necessary and identify by block number)

We report in-situ surface X-ray scattering measurements of electrochemically deposited TI monolayers on Ag(III). We find that the TI adlayer forms an incommensurate, two dimensional solid and we determine the spatial modulation in the TI monolayer that is induced by the periodict potential of the substrate. The modulation of the TI monolayer changes the intensity of the X-ray scattering from the Ag substrate (the Ag crystal truncation rods), since the modulation wavevectors are commensurate with the substrate periodicity. By measuring the intensity changes along the Ag truncation rods, we determined the first Fourier component of the longitudinal part of the substrate induced modulatioin to be 0.03Å, and the spacing of the TI

20 DISTRIBUTION / AVAILABILITY OF ABSTRACT ☑ UNCLASSIFIED/UNLIMITED ☐ SAME AS RPT ☐ DTIC USERS	21 ABSTRACT SECURITY CLASSIFICATION
22a NAME OF RESPONSIBLE INDIVIDUAL Dr. Robert J. Nowak	22b TELEPHONE (Include Area Code) (202) 696-4410	22c. OFFICE SYMBOL ONR 472

DD FORM 1473 84 MAR   83 APR edition may be used until exhausted

monolayer above the Ag surface to be 3.05Å. In addition, from the phase of teh monolayer scattering amplitude (relative to the substrate scattering amplitude) required to fit the data, the lowest energy sites on the surface are identified as the three-fold hollow sites. Using the Novaco-McTague model and estimates of the elastic susceptibility of the TI monolayer, we also estimate the first Fourier component of the surface energy corrugation to be 2-3meV (0.05-0.07kal/molc). To obtain the modulation amplitude, we have analyzed the ratio of the Ag truncation rod intensities with and without the monolayer rather than the intensities. The use of this 'ratio' method was very important because the ratio is considerably more accurate than the intensities. We also find that the bare Ag(III) surface in contact with electrolyte is very flat (an rms roughness of 0.7Å) compared to similar metal surfaces prepared by sputtering and annealing in vacuum (rms roughness ~3-5Å).

Accession For	
NTIS GRA&I	☑
DTIC TAB	☐
Unannounced	☐
Justification	
By	
Distribution/	
Availability Codes	
Dist	Avail and/or Special
A-1	

Research Report

SURFACE X-RAY SCATTERING MEASUREMENTS OF THE
SUBSTRATE INDUCED SPATIAL MODULATION OF AN
INCOMMENSURATE ADSORBED MONOLAYER

Michael F. Toney
Joseph G. Gordon
Mahesh G. Samant
Gary L. Borges
Owen R. Melroy
Lung-Shan Kau
David G. Wiesler

IBM Research Division
Almaden Research Center
650 Harry Road
San Jose, California 95120-6099

Dennis Yee
Larry B. Sorensen
Department of Physics FM-15
University of Washington
Seattle, Washington 98195

Surface x-ray scattering measurements of the substrate induced spatial modulation of an incommensurate adsorbed monolayer

Michael F. Toney, Joseph G. Gordon, Mahesh G. Samant, Gary L. Borges,
Owen R. Melroy, Lung-Shan Kau, David G. Wiesler
IBM Research Division
IBM Almaden Research Center
650 Harry Road
San Jose, CA 95120

Dennis Yee and Larry B. Sorensen
Department of Physics FM-15
University of Washington
Seattle, WA 98195

Abstract

We report in-situ surface x-ray scattering measurements of electrochemically deposited Tl monolayers on Ag(111). We find that the Tl adlayer forms an incommensurate, two dimensional solid and we determine the spatial modulation in the Tl monolayer that is induced by the periodic potential of the substrate. The modulation of the Tl monolayer changes the intensity of the x-ray scattering from the Ag substrate (the Ag crystal truncation rods), since the modulation wavevectors are commensurate with the substrate periodicity. By measuring the intensity changes along the Ag truncation rods, we determined the first Fourier component of the longitudinal part of the substrate induced modulation to be 0.03 Å, and the spacing of the Tl monolayer above the Ag surface to be 3.05 Å. In addition, from the phase of the monolayer scattering amplitude (relative to the substrate scattering amplitude) required to fit the data, the lowest energy sites on the surface are identified as the three-fold hollow sites. Using the Novaco-McTague model and estimates of the elastic susceptibility of the Tl monolayer, we also estimate the first Fourier component of the surface energy corrugation to be 2-3meV (0.05-0.07kcal/mole). To obtain the modulation amplitude, we have analyzed the ratio of the Ag truncation rod intensities with and without the monolayer rather than the intensities. The use of this 'ratio' method was very important because the ratio is considerably more accurate than the intensities. We also find that the bare Ag(111) surface in contact with electrolyte is very flat (an rms roughness of 0.7Å) compared to similar metal surfaces prepared by sputtering and annealing in vacuum (rms roughness ~3-5Å).

I. Introduction

The periodic potential of a substrate has important influences on the crystallographic structure, lattice constants and orientation of thin films that are grown on it. When the adsorbate-substrate interactions are much stronger than the adsorbate-adsorbate interactions (i.e. the strong substrate limit), the substrate periodicity dictates the structure of the thin adsorbed film. This results in the formation of a commensurate or registered film and psuedomorphic growth. If the adsorbate-substrate interactions are much weaker than the adsorbate-adsorbate interactions (i.e. the weak substrate limit), then the thin film assumes an incommensurate structure that is much closer to the crystallographic structure it would assume if the substrate were absent. However, the substrate still has some influence, since its periodic potential creates small amplitude static displacements in the atomic positions of the thin adsorbed layer.[1,2] This static distortion wave (or substrate-induced spatial modulation) can lead to a rotation of the adsorbed layer with respect to the substrate, as predicted by Novaco and McTague (NM),[3,4] and to commensurate-incommensurate phase transitions,[5] if the ratio of the adsorbate-adsorbate to substrate-adsorbate interactions can be varied. Because the substrate-induced modulation has Fourier components (i.e. wavevectors) that are commensurate with the substrate periodicity, the scattering from the adsorbed layer interferes coherently with scattering from the substrate. Thus, the adsorption of the thin film changes the apparent intensity of the substrate diffraction.

We have observed this effect by measuring the surface x-ray scattering (crystal truncation rods) from Ag(111) substrates with and without a monolayer of Tl. The Tl is deposited (and removed) electrochemically and forms an ordered, incommensurate, hexagonal monolayer. The measurements were conducted in-situ (in contact with the electrolyte) and under potential control. From the ratio of the truncation rod intensities with and without the monolayer, we have determined that the longitudinal part of the

first Fourier component of the substrate induced modulation is 0.03Å and that the average spacing of the Tl monolayer above the Ag surface is 3.05Å. In addition, the phase of the monolayer scattering amplitude was determined and shows that the lowest energy positions on the surface are the three-fold hollow sites. The use of the intensity ratio was very important, since the ratio is more accurate than the intensities. By using the NM model[3, 4] and estimates of the elastic response of the Tl monolayer, we have also estimated the first Fourier component of the surface energy corrugation as 2-3meV (0.05-0.07kcal/mole).

The remainder of the paper is organized as follows. In Section II we first discuss substrate-induced spatial modulation of adlayers and then calculate how this modifies the scattering intensity at the substrate diffraction wavevectors. In Section III the experimental details are outlined. The electrochemical deposition of Tl on Ag(111), the surface scattering data (including the necessary experimental corrections), and the data analysis are discussed in Section IV. In Section V our estimate of the surface potential energy corrugation is described and our results are discussed and compared with other measurements.[6-9] The final section contains concluding remarks.

II. Substrate-Induced Spatial Modulation of Adlayers

Figure 1 illustrates, in a one dimensional model, the origin of the substrate-induced spatial modulation in an adsorbed monolayer.[1, 2] Although the adlayer is incommensurate with the substrate, its energy is reduced when the local positions of the adatoms shift slightly as they tend to move toward positions of lower energy. These shifts are the substrate-induced spatial modulation, $\vec{u}_j$, and they have the same periodicity as the substrate. Thus, denoting the position of the jth adatom in the absence of the substrate as $\vec{R}_j$, the modulation can be expanded in terms of the substrate wavevectors,

$$\vec{u}_j = \sum_{\vec{G}} \vec{u}_{\vec{G}} \, \exp(i\vec{G} \cdot \vec{R}_j), \tag{1}$$

where $\vec{G}$ is a reciprocal lattice vector of the substrate surface (in the plane of the surface) and $\vec{u}_{\vec{G}}$ is the amplitude of the modulation with wavevector $\vec{G}$.[3, 4, 10] The magnitude of $\vec{u}_{\vec{G}}$ is determined by the lattice mismatch between the adsorbate and substrate and by the ratio of the adsorbate-adsorbate to adsorbate-substrate interaction potentials. The modulation will be small if the adatom-substrate potential is weak compared to the adatom-adatom potential and the adlayer lattice spacing does not closely match the substrate lattice. If the reverse are true, $\vec{u}_{\vec{G}}$ will be large.

We have made the assumption in Equation (1) that the modulation $\vec{u}_j$ is small, and hence, the adlayer response to the substrate potential is linear. Our results will demonstrate that this approximation is valid. We also assume, as is usually the case,[3, 4, 10] that the modulation normal to the surface is negligibly small. In addition, we assume only the lowest order set of symmetry equivalent $\{\vec{G}\}$ contributes to the sum in Equation (1), since the amplitudes $\vec{u}_{\vec{G}}$ with these wavevectors are small and higher order harmonics are likely smaller. Since the modulation is centro-symmetric ($\vec{u}_j = -\vec{u}_{-j}$), we choose the real-space origin to be a substrate site, so that $\vec{u}_{\vec{G}}$ is purely imaginary.

The scattering amplitude for the modulated incommensurate layer at scattering vector $\vec{Q}$ is

$$A_m(\vec{Q}) = F_m(\vec{Q}) \sum_j \exp\left[-i\vec{Q} \cdot (\vec{R}_j + \vec{u}_j) \right]$$

$$\simeq F_m(\vec{Q}) \sum_j \left[(1 - i\vec{Q} \cdot \vec{u}_j) \right] \exp(-i\vec{Q} \cdot \vec{R}_j), \tag{2}$$

where F_m is the atomic scattering factor of the adatoms and we have again assumed the modulation is small. Substituting the expression for the modulation $\vec{u}_j$ (Equation (1)) into Equation (2), yields

$$A_m(\vec{Q}) = N_m F_m(\vec{Q}) \left[\sum_{\vec{\tau}} \delta(\vec{Q}_\parallel - \vec{\tau}) - i \sum_{\vec{\tau}} \sum_{\vec{G}} (\vec{Q} \cdot \vec{u}_{\vec{G}}) \delta(\vec{Q}_\parallel - (\vec{G} - \vec{\tau})) \right], \quad (3)$$

where δ is the Dirac delta, $\vec{\tau}$ is a reciprocal lattice vector of the unmodulated incommensurate adlayer, $\vec{Q}_\parallel$ is the component of $\vec{Q}$ parallel to the surface, and N_m is the total number of atoms in the adlayer. The leading term represents the main diffraction peaks at the adlayer reciprocal lattice vectors. The second term represents the 'modulation superlattice' diffraction peaks (also know as 'satellite' peaks), which are found at $\vec{Q}_\parallel = \{\vec{G}\} - \{\vec{\tau}\}$. These have been observed for strongly modulated adlayers, such as Kr on graphite;[9] similar satellites have also been observed in three dimensional (3D) materials when the atom positions are modulated with a periodicity that is incommensurate with the 3D lattice.[11-13] In this paper we concentrate on the adlayer scattering with $\vec{\tau} = 0$, which occurs at the substrate-surface reciprocal lattice vectors $\vec{Q}_\parallel = \vec{G}$, and hence, interferes with the scattering from the substrate. Because the scattering amplitude from a monolayer is of the order N_m, this interference is only important when the substrate scattering is of the same order; this occurs near the anti-nodes of the substrate crystal truncation rods.

The termination of a crystal at a surface or interface gives rise to tails of intensity about bulk Bragg points extending along directions normal to the surface.[14-17] If we take the z-direction as along the surface normal, this scattering occurs along a rod such that $\vec{Q} = \vec{G} + Q_z \hat{z}$, where Q_z is the component of the scattering vector in the z-direction and $\hat{z}$ is the unit vector in that direction. These rods of scattering have been termed crystal truncation rods (CTRs).[14] The CTR amplitude for a perfectly flat (111) face-centered cubic (fcc) crystal is[14, 18]

$$A_s(\vec{Q}) = \frac{N_s \, F_s(\vec{Q})}{1 - \exp iK} , \tag{4}$$

where $K = (2\pi/3)(h - k) + CQ_z$, C : the layer spacing, N_s is the number of atoms in a single (111) layer of the substrate, and F_s is the atomic scattering factor of the substrate atoms. We have adopted a hexagonal unit cell (denoted h) for the fcc crystal so that

$$(100)_h = \tfrac{1}{3}(4\overline{2}\overline{2})_c \quad (010)_h = \tfrac{1}{3}(22\overline{4})_c \quad (001)_h = \tfrac{1}{3}(111)_c, \tag{5}$$

where c refers to the cubic unit cell.

The total CTR scattering amplitude, A, for a modulated, incommensurate adlayer adsorbed on an undistorted substrate is the sum of the amplitudes from the bare substrate and the adlayer:[19]

$$A(\vec{Q}) = A_s + A_m = \frac{N_s \, F_s(\vec{Q})}{1 - \exp iK} - iN_m F_m(\vec{Q})(\vec{G} \cdot \vec{u}_{\vec{G}}) \exp(-idQ_z), \tag{6}$$

where d is the average (center-to-center) spacing of the monolayer above the top layer of the substrate. Because $\vec{u}_{\vec{G}}$ is imaginary, the phase of the adlayer scattering (the phase of the second term) is either 0 or π when $Q_z = 0$. Since the interference between the adlayer and the substrate scattering changes the CTR amplitude, measurements of the CTR intensity can be used to determine the longitudinal Fourier components of the modulation ($\vec{G} \cdot \vec{u}_{\vec{G}}$) and the substrate-monolayer separation, d.

Until now, we have implicitly assumed that the substrate surface is perfectly flat. Of course, real surfaces are not perfectly flat but have atomic scale roughness (e.g. steps). This roughness is included in our analysis in a convenient way by using a simple, real-space model introduced by Robinson.[14] In this model, partially filled layers are

added to the surface and each added layer has a fractional occupancy β $(0 < \beta < 1)$. This model can account for stepped surfaces and with it the CTR intensity $I = |A|^2$ becomes

$$I = \frac{(1 - \beta)^2}{1 + \beta^2 - 2\beta \cos K} \left| \frac{N_s F_s(\vec{Q})}{1 - \exp iK} - iN_m F_m(\vec{Q})(\vec{G} \cdot \vec{u}_{\vec{G}}) \exp(-idQ_z) \right|^2 . \qquad (7)$$

Here $\beta = 0$ represents a perfectly flat surface, while $\beta = 1$ is infinitely rough. It is perhaps more physical to think of the surface roughness in terms of an root-mean-square (rms) roughness, which in this fractional-occupancy model is $(\sqrt{\beta}/(1 - \beta))C$.[14] Recall that C is the layer spacing.

The fractional-occupancy model is only one of several that can describe an imperfect surface. CTR data have been successfully fit with other models that do not have a rough (e.g. stepped) surface but have enhanced disorder in the topmost substrate layer.[15, 20] These models describe the disorder with an enhanced Debye-Waller factor. The fit to our data with these models is essentially the same as that using the fractional-occupancy model and we cannot distinguish between the various models. We use the fractional-occupancy model solely for convenience.

III. Experimental

All of our experiments were performed in-situ (in electrolyte), under potential control, and at room temperature. The electrochemical cell is essentially the same as that used to investigate electrochemically deposited Pb on Ag(111)$_c$ and Au(111)$_c$ and has been described in detail.[21, 22] To prevent oxidation of the monolayer caused by diffusion of atmospheric O_2 to the surface, we flow Ar gas through a cylindrical Kapton window that surrounds the electrode. With this arrangement, no changes in the diffraction pattern from the monolayer were observed over a period of one day. The electrode substrates were epitaxially grown thin films of Ag that were vapor deposited onto freshly cleaved mica[21, 22] and the electrolyte was 0.1M Na_2SO_4 containing 2.5mM Tl_2SO_4. The Tl

monolayer was deposited with the cell inflated so a relatively thick (~1mm) layer of electrolyte covers the electrode. The electrolyte was then partially removed and the diffraction data were measured through a thin ($\lesssim 30\mu$m) layer of electrolyte. All potentials are reported relative to the Ag/AgCl (3M KCl) reference electrode.

The data were collected at the National Synchrotron Light Source (NSLS) beam line X20A.[23] An incident x-ray energy of 9997 eV (1.240Å) was selected using a Si(111) double monochromator. At the sample the focused x-ray beam had a vertical and horizontal full-width at half-maximum (FWHM) of 0.8mm and 1.7mm, respectively. The incident beam intensity was monitored by a NaI scintillation detector viewing a Kapton beam splitter. The diffracted beam was analyzed with 1mrad Soller slits and the intensity was measured with a NaI scintillation detector. The sample was aligned using the bulk Ag $(101)_h$ and $(011)_h$ reflections; all data are obtained in the symmetric ($\omega = 0$) mode.[24]

IV. Results

Before describing our x-ray measurements, we first discuss the underpotential electrochemical deposition of Tl on $Ag(111)_c$. Electrochemical deposition of metal layers onto a foreign metal substrate frequently occurs in distinct stages with the initial formation of one (or more) layers at electrode potentials positive of the reversible thermodynamic (Nernst) potential for bulk deposition.[25, 26] This process is thus termed underpotential deposition (UPD). On single crystals, these initial deposits are believed to be well defined, ordered layers.[27] The UPD layers are frequently deposited by linearly sweeping the electrode potential in the negative direction from a suitable positive potential. Figure 2 shows a typical current response of the Ag electrode to a linear potential sweep (a cyclic voltammogram) for Tl on $Ag(111)_c$.[28, 29] If the adsorbing ion is completely discharged (as for $Tl/Ag(111)_c$[28]) and kinetic effects are absent, the current response is proportional to the derivative of the adsorption isotherm.[30]

The predominant features in Fig. 2 are two large, sharp peaks. The first, at approximately -470mV (240mV positive of the reversible Nernst potential) has previously been attributed to the deposition of a single monolayer of Tl.[28, 30, 31] As will be reported elsewhere,[32] our in-situ surface x-ray scattering measurements of this Tl layer show that it is a two dimensional (2D), incommensurate hexagonal solid, slightly compressed from the bulk metal and rotated about 4-5° from the Ag $(100)_h$ direction. The second peak in Fig. 2 corresponds to the deposition of a second layer of Tl on top of the first, forming a bilayer where the two layers are mutually commensurate. Like the monolayer, the bilayer is also incommensurate with the Ag substrate and has a hexagonal structure that is slightly compressed from the bulk metal (although less than the monolayer) and is rotated about 4° from the Ag $(100)_h$ direction.[32]

Figures 3(a) and (b) show, respectively, the intensities of the Ag $(10Q_z)_h$ rods with and without the Tl monolayer present. These data were obtained by measuring the peak intensity and subtracting the background (which was obtained at an azimuthal angle 1° from the peak). To compare the data with the calculated CTR intensity (Eq. (7)), the data have been corrected for active sample area, Lorentz factor, Ag scattering factor, and resolution function. The sample area and resolution function corrections will be described in detail elsewhere.[32] Briefly, the resolution function correction accounts for the overlap between the surface scattering and the highly anisotropic resolution volume associated with our scattering geometry.[33, 34] The anisotropic resolution volume tilts as a scan is made along the CTR, resulting in a decreasing overlap with increasing Q_z. To correct the experimental data for this, the shape of the resolution volume must be known. We have made careful scans at several points along the CTR and fit these to a resolution volume that has a broad 'slit-like' shape in the out-of-plane direction (FWHM = 0.12Å^{-1}) and a sharper shape in the in-plane direction.[32] When convoluted with the finite size of the Ag surface domains, the in-plane peak shape is conveniently fit with a Lorentzian squared (FWHM = 0.016Å^{-1}),[32] although we attach no physical significance to this fit. The experimental data are corrected using this measured, anisotropic

reciprocal-space volume (i.e. a 0.12Å^{-1} 'slit-like' out-of-plane shape and a 0.016Å^{-1} Lorentzian-squared in-plane shape). The sample area correction accounts for the fact that at small α all of the sample is illuminated, while at larger α only a portion (essentially proportional to $\sin\alpha$) is illuminated. This correction is made using the measured beam shape. We estimate that when the experimental data have been corrected for sample area, Lorentz factor, Ag scattering factor, and resolution function they are accurate to about 5%. This uncertainty is due to inaccurate knowledge of the area and resolution function corrections.[32]

The data from the Ag substrate without the Tl monolayer were fit to the CTR intensity of a bare substrate with some roughness. The CTR intensity was modeled using Equation (7) with $N_m = 0$ and four fitting parameters: 1) the roughness factor β;[14] 2) an overall scale factor; 3) the x-ray absorption due to the electrolyte and polypropylene film covering the Ag electrode; and 4) the fraction of CBA (relative to ABC) stacking in the substrate. The latter parameter is necessary because the vapor deposited Ag thin films used in this work have both ABC and CBA stacking. Consequently, the rod scans shown in Figure 3 contain contributions from both the $(10Q_z)_h$ and the $(01Q_z)_h$ Ag CTRs. Since the contributions are not equal, the relative fractions of each stacking sequence must also be fit to the data. For the data shown in Figure 3, the best fit gives 0.62 ABC and 0.38 CBA. This fraction can be checked by measurements of the intensities of the $(102)_h$ and $(011)_h$ bulk Bragg peaks and those Bragg peaks rotated 60° from these; we found that this gave a consistent result. Similar fractions are found for several other Ag films.[35]

The x-ray absorption of the material covering the electrode reduces the observed intensity by $\exp - (2\mu t / \sin\alpha)$, where α is the incidence angle and $2\mu t$ is the absorption of the incident and diffracted x-rays by the polypropylene film and the electrolyte. In these experiments, the angular collimation in the out-of-plane direction was (purposely) rather poor ($\simeq 1.4°$), which results in a fairly large spread in exit angles. Thus, the ab-

sorption correction must be integrated over this range of exit angles. This effect was taken into account when fitting the data, but is only important at small Q_z. Since the thickness and composition of the polypropylene film are known and the composition of the electrolyte is also known, we can estimate the electrolyte thickness from the value of μt. The best fit value is $\mu t = 0.016$, which yields an electrolyte thickness of $30\mu m$.

The best fit to the CTR intensity for the bare Ag substrate is shown by the solid line in Figure 3(a). The fit is quite good for most Q_z; however, it is not very good at small Q_z ($\lesssim 0.3$). This discrepancy is probably caused by nonuniformities in the thickness of the electrolyte layer. The absorption correction is highly nonlinear at small Q_z (since it is an exponential of (electrolyte thickness)/Q_z). Thus, a fraction of the sample with an electrolyte thickness that is slightly smaller than average will disproportionally contribute to the measured intensity at small Q_z. This effect is not accounted for with the simple correction given above, since the electrolyte thickness is assumed to be uniform. At larger Q_z the correction becomes much more linear and the effect of nonuniformities becomes much smaller. Consequently, the data are only fit for $Q_z > 0.3$.

The best fit to the data for the bare surface yields a value of $\beta = 0.08\pm0.02$ or an rms roughness of 0.7Å. This small value shows that the Ag substrates in contact with this electrolyte are quite smooth. Indeed, this surface is much smoother than similar metal surfaces prepared by sputtering and annealing in a vacuum environment, which have $\beta \sim 0.5 - 0.7$ or rms roughness of 3-5Å.[14, 20] This suggests that the Ag surface is inherently smooth in an aqueous environment at this potential (-200mV, well negative of the dissolution potential).

Figure 3(c) shows the ratio of the CTR intensity with the Tl monolayer present (V = -600mV) to that with the monolayer (V = -200mV) absent. By taking this ratio, the instrumental corrections and the solution absorption correction cancel; thus, the uncertainty in the ratio is considerably smaller than the uncertainties for the intensities. The

ratio shows that when the monolayer is adsorbed the CTR intensity is decreased for $Q_z \lesssim 1$, but increased slightly for $Q_z \gtrsim 1$. This change cannot be explained simply by an increase in surface roughness, since this would decrease the CTR intensity at all Q_z. However, the change is consistent with that expected for the adsorption of a spatially-modulated incommensurate monolayer on the Ag substrate. This monolayer-present ($N_m \neq 0$) to monolayer-absent ($N_m = 0$) ratio is calculated using the expression for CTR intensities (Equation (7)):

$$R = \left| 1 - i \frac{(1 - \exp iK) N_m F_m(\vec{Q})(\vec{G} \cdot \vec{u}_{\vec{G}}) \exp(-idQ_z)}{N_s F_s(\vec{Q})} \right|^2 , \qquad (8)$$

where $\vec{G}$ is the Ag $(100)_h$ reciprocal lattice vector.

The best fit of the CTR intensity ratio to Equation (8) is shown by the solid line in Figure 3(c). The fit is excellent over most of the data range. The slight deviation from the data for $Q_z \simeq 0 - 0.15$ is probably caused by very small changes in the nonuniformities in solution thickness as discussed above. Only two parameters were used in this fit: the Ag-Tl spacing, d, and the the first longitudinal Fourier component of the modulation, $u_{\vec{G}}^l \equiv i(\vec{u}_{\vec{G}} \cdot \vec{G})/|\vec{G}|$ for $\vec{G} = (100)_h$. The overall scale factor, electrolyte absorption, and roughness β were all assumed to be the same as for the bare substrate and are thus canceled out by taking the ratio. In addition, we use the fraction of CBA stacking determined from the fit to the bare Ag substrate. The line in Figure 3(b) shows the corresponding CTR intensity with the Tl monolayer present; this is calculated using these same values of β, scale factor, electrolyte absorption, CBA stacking fraction, and the best-fit values of $u_{\vec{G}}^l(\vec{G} = (100)_h)$ and d. The agreement between the calculated intensity and the data is very good and is comparable to that in Figure 3(a).

In the best fit the first Fourier component of the substrate induced modulation in the incommensurate Tl monolayer is $u_{\vec{G}}^l(\vec{G} = (100)_h) = +0.031 \pm 0.005$Å. This is a small modulation compared to the 3.34Å near-neighbor spacing of the Tl monolayer[32] and

validates our assumption that the modulation is small enough so the adlayer responds linearly to the substrate potential. An adequate fit is obtained only if the relative phase between the substrate and monolayer scattering is 0 (u_G^l is positive). Since the real-space origin is chosen as an Ag atom in the top layer, this shows that the adatoms prefer to move away from the on-top sites and towards three-fold hollow sites. When the unmodulated position $\vec{R}_j$ is close to an on-top site ($\vec{G} \cdot \vec{R}_j \simeq 2n\pi$, $n=$ integer), the exponential in the expression for the modulation $\vec{u}_j$ (Equation (1)) can be approximated as $\exp(i\vec{G} \cdot \vec{R}_j) = 1 + i(\vec{G} \cdot \vec{R}_j - 2n\pi)$. When this is used in Equation (1) and use is made of the symmetry relation $\vec{u}_{\vec{G}} = -\vec{u}_{-\vec{G}}$ (i.e. $\vec{u}_j$ is real) and the fact that $\vec{u}_{\vec{G}}$ imaginary, one can see that the adatoms tend to shift away from the on-top sites. An analogous argument applies when $\vec{R}_j$ is close to a three-fold hollow ($\vec{G} \cdot \vec{R}_j \simeq (2n + 1)\pi \pm \pi/3$). As we show below, this preferred motion is reasonable, since the potential energy minima are the three-fold hollow sites.

The best fit value for the average spacing between monolayer and substrate is 3.05±0.1Å. For an incommensurate adlayer it is not immediately obvious that one can determine this spacing by measuring the off-specular ($Q_\parallel \neq 0$) scattering from the substrate (or even that an incommensurate adlayer will change the off-specular scattering from the substrate at all). However, the existence of the substrate-induced spatial modulation in the adlayer makes this measurement possible, since the modulation wavevectors are commensurate with the substrate periodicity.

The CTR intensities with and without the Tl monolayer were also measured on a different substrate than that used for the data shown in Fig. 3. Although the uncertainties in these data are larger than those in Fig. 3, they were also analyzed as described above. The results for the modulation, Tl-Ag spacing, and surface roughness are, respectively, $u_G^l = 0.034$Å, $d = 3.15$Å, and $\beta = 0.10$ (an rms roughness of 0.8Å). These values are all within estimated errors quoted above, which gives us confidence that our results are correct. The solution thickness, however, is slightly smaller, 20μm compared to

30μm. This is likely due to a different azimuthal orientation of the clip that retains the substrate or a slightly different tension on the polypropylene film covering the electrode.[21, 22]

V. Discussion

We have determined the substrate-induced modulation of an incommensurate Tl monolayer, by measuring the ratio of the Ag $(100)_h$ CTR with and without the monolayer adsorbed. It is important to note that in this 'ratio method' all the instrumental corrections cancel out exactly, and for a given Ag substrate, the solution absorption correction also cancels. Thus, there is no uncertainty in the ratio due to inaccurate knowledge of the sample area correction or the resolution function correction. We estimate that the accuracy of the ratio is about 1.5%, based on the reproducibility of these data. This is limited primarily by counting statistics and small displacements of the Ag substrate that occur when the electrolyte is added and removed from the cell during the deposition process. This accuracy compares favorably to the estimated 5% error in the intensity data. The ratio method is, thus, extremely effective and was essential for these measurements.

Although we are able to fit the data in Figure 3 quite well with a CTR intensity due to a substrate-modulated incommensurate layer, other explanations are possible. As mentioned above, the decrease in CTR intensity at small Q_z and increase at large Q_z cannot be explained by a change in surface roughness (either with different β or with enhanced disorder in the top substrate layer). A model with large changes in the interlayer spacings between the top three Ag layers (relaxation of these layers) can fit the data. However, the required changes are much too large (0.1-0.2Å) to be physically reasonable. For (111) surfaces of fcc crystals, the first layer relaxation is generally $\lesssim 0.02$Å and deeper layers do not relax.[36] We have also checked the assumption that the surface roughness (described by β) does not change when the Tl monolayer is adsorbed.

The fit to the ratio in Fig. 3(c) is not improved if β is allowed to vary as a fitting parameter. This demonstrates that the substrate does not become significantly rougher when the UPD monolayer is adsorbed.

The substrate-induced spatial modulation is directly related to the elastic response of the incommensurate layer and to the substrate potential energy corrugation - if the adlayer is soft and the energy corrugation is large, then the modulation will be large. This argument is qualitative. We can obtain a semi-quantitative estimate of the substrate corrugation by using the model developed by NM[3, 4] together with an estimate of the elastic response of the adlayer. NM calculate the energy change of the adlayer due to the creation of a periodic, substrate-induced spatial modulation. This energy is minimized when the adlayer is rotated away from high symmetry directions of the substrate and the model predicts the rotation angle of the adlayer, which depends on the adlayer lattice spacing. The following approximations are made in the NM model: i) the interaction between adatoms is harmonic, ii) the substrate is rigid, iii) thermal effects are not important (the temperature is zero), and iv) the substrate-induced spatial modulation is small. We have shown that approximation (iv) is correct, but have no evidence regarding the first three.

For Ti[32] and Pb[21, 22, 37, 38] on Ag(111)$_c$, the NM model predicts rotation angles (from the Ag(100)$_h$ direction) of $\simeq 5°$ and $\simeq 5.5°$, respectively, which are within about a degree of what we measure. However, we do not observe any dependence of the rotation angle on lattice spacing,[21, 22, 32, 37, 38] in apparent disagreement with the NM model. One conceivable cause of the discrepancy is a small amount of impurity adsorption during the experiment,[32] since small quantities of adsorbed impurities have been shown to influence the rotation angle.[39] There are, however, several other possible explanations.[21, 22, 38] Keeping in mind the uncertainties due to this discrepancy and the unknown validity of the approximations used in the NM model, we will use this model to

estimate the substrate potential energy corrugation. We emphasize that this is only an estimate.

With the above approximations, NM calculate $\vec{u}_{\vec{G}}$ as[4]

$$\vec{u}_{\vec{G}} = -i \sum_k \frac{(\vec{\varepsilon}_k(\vec{G}) \cdot \vec{G})}{M\omega_k^2(\vec{G})} \, V_{\vec{G}} \, \vec{\varepsilon}_k(\vec{G}). \tag{9}$$

Here M is the adatom mass and $\omega_k(\vec{G})$ and $\vec{\varepsilon}_k(\vec{G})$ are, respectively, the frequencies and polarization vectors of the phonons in the adlayer and k is the phonon mode label (longitudinal or transverse). The adsorbate-substrate interaction potential $V(\vec{r})$ has been decomposed into Fourier components[40]

$$V(\vec{r}) = \sum_{\vec{G}} V_{\vec{G}} \, \exp(i\vec{G} \cdot \vec{r}). \tag{10}$$

In the long wavelength limit, the relationship between $u_{\vec{G}}^l$ to $V_{\vec{G}}$ (Equation (9)), becomes[4]

$$u_{\vec{G}}^l = \frac{V_{\vec{G}}}{GMc_T^2} \left[\frac{1}{1 + z^2 - 2z\cos\Omega} + \frac{\eta z^2 (\sin\Omega)^2}{(1 + z^2 - 2z\cos\Omega)^2} \right], \tag{11}$$

where $\eta = (c_L/c_T)^2 - 1$ and c_L and c_T are the adlayer longitudinal and transverse sound velocities, respectively. The rotational epitaxy angle, Ω, is the angle between the substrate and adsorbate reciprocal lattice vectors, $\vec{G}$ and $\vec{\tau}$, respectively, and $z = \tau/G$. For Tl/Ag(111)$_c$, $\vec{G}$ and $\vec{\tau}$ are the lowest order reciprocal lattice vectors.

To calculate $V_{\vec{G}}$ from Equation (11), it is necessary to determine the longitudinal and transverse sound velocities for the Tl monolayer. Although these have not been measured, we can estimate them by using two models. In the simplest, we calculate the sound velocities of a very thin plate of Tl[41] using the bulk, isotropic values of Young's

modulus E and Poisson's ratio σ.[42, 43] This yields $c_l = 1.4 \times 10^5$ cm/sec and $c_t = 4.8 \times 10^4$ cm/sec. An alternate approach that approximately takes into account the anisotropy of Tl force constants is to model the monolayer as a very thin plate of Tl with the (001) direction normal to the plate. The in-plane values of E and σ are calculated[42] from the bulk Tl elastic constants[43] and are used to estimate the sound velocities for the thin plate.[41] The result is $c_l = 9.3 \times 10^4$ cm/sec and $c_t = 4.8 \times 10^4$ cm/sec. Both these models do not correctly treat the anisotropy of the force constants and ignore the fact that these are different in a monolayer than in bulk. They are, however, adequate for our purpose. Using these sound velocity values, we estimate that the first Fourier component of the energy corrugation is $V_{\vec{G}}(\vec{G} = (100)_h) = 2\text{-}3\text{meV}$ (0.05-0.07kcal/mole). We note that this is the corrugation energy for an atom *in a monolayer* when it is surrounded by other Tl adatoms. This energy is probably not the same as that for an isolated adatom due the metallic bonding in the monolayer.

The estimated value of $V_{\vec{G}}(\vec{G} = (100)_h) = 2\text{-}3\text{meV}$ is about 0.1% of the estimated 2eV bond energy between Tl and Ag. (The bond energy is estimated as the sum of the cohesive energy of bulk Tl plus the UPD shift).[25] We are unaware of any theoretical predictions or other measured values of $V_{\vec{G}}$ for metals adsorbed on other metals, and so, it is difficult to compare this value to others. However, it is reasonable to compare $3V_{\vec{G}}$ to the activation energy for surface diffusion E_d, since these are both the energy required for an adatom to pass from the potential minimum to the potential saddle point. In general, for metals adsorbed in vacuum onto other metals E_d is a few tenths of an eV or more,[44] significantly larger than $3V_{\vec{G}}$. We speculate that this results because the diffusion measurements are made for isolated adatoms, while the corrugation energy we measure is for an adatom *within* a monolayer. Perhaps the metallic bonding between the adatoms within the monolayer reduces the energy corrugation caused by the substrate potential.

The best-fit center-to-center spacing between the Tl monolayer and the Ag substrate is 3.05Å. This average separation is slightly smaller than the 3.16Å spacing obtained by simply placing a rigid close-packed layer of Tl atoms (radius $\simeq 1.72$Å) above a rigid close-packed layer of Ag atoms (radius $\simeq 1.44$Å). Although the estimated accuracy of our determination (± 0.1Å) makes it impossible to be certain that this difference is real, a smaller spacing is certainly reasonable. The smaller spacing could result because most of the adatoms are not directly above Ag atoms; instead, they are near hollow and bridge sites where they are closer to the top Ag layer. Alternatively, the strong attraction between the adsorbate and substrate could cause this reduction. Or the very large electric field present at this electrode-electrolyte interface may influence the attraction and also affect this distance. It will be interesting to see how the Ag-Tl spacing changes with applied potential. As mentioned earlier, we have assumed that the modulation normal to the surface is negligibly small. A fit to the ratio data in Fig. 3(c) with a non-zero normal modulation did not result in an improved fit compared to the fit with zero normal modulation. To determine this modulation, it will be necessary to obtain data to much larger Q_z.

The maxima and minima of the substrate-adsorbate interaction potential are easily calculated from the expression for $V(\vec{r})$ (Equation (10)). Since $V_{\vec{G}}$ is positive, the maxima occur at substrate positions $\vec{r}$ such that $\vec{G} \cdot \vec{r} = 2n\pi$ (n = integer); these are sites directly above Ag atoms. The interaction energy minima are at the three-fold hollow sites, since these sites have $\vec{G} \cdot \vec{r} = (2n+1)\pi \pm \pi/3$ and minimize Equation (10). It is not surprising that the three-fold hollow sites are the minimum energy sites for Tl on Ag(111), because at these sites the adatoms have maximum coordination. Indeed, in the vacuum deposition of Tl on Ag(111), a low coverage $(\sqrt{3} \times \sqrt{3})R30°$ structure is observed and in the proposed model for this structure, all the adatoms occupy three-fold hollow sites.[45]

To construct a real-space picture of the modulated Tl monolayer, the transverse component of the spatial modulation, $u_{\vec{G}}^t = \vec{u}_{\vec{G}} - u_{\vec{G}}^l(\vec{G}/G) = \vec{u}_{\vec{G}} \cdot (\hat{z} \times \vec{G})/G$, must be determined. Since x-ray scattering measures $\vec{G} \cdot \vec{u}_j$, we cannot directly measure this transverse modulation. However, by using the NM expression for $\vec{u}_{\vec{G}}$ (Equation (9)) and our estimate for $V_{\vec{G}}$, the transverse modulation is estimated as $u_{\vec{G}}^t = 0.022\text{Å}$, which is slightly smaller than $u_{\vec{G}}^l$.

Figure 4 shows several schematic representations of the real space structure of one domain of Tl on Ag(111). For comparative purposes, the hypothetical *unmodulated* adlayer is shown in Fig. 4(a). The open circles represent atoms of the Ag(111) surface and have a diameter equal to their nearest-neighbor spacing (2.89Å). The shaded circles represent the Tl adatoms and have a diameter of 3.34Å, which is their average nearest-neighbor spacing.[32] Using the measured $u_{\vec{G}}^l$ and the estimated $u_{\vec{G}}^t$, the modulated positions of the adatoms in the monolayer are calculated using Equation (1) and are shown in Fig. 4(b). A comparison of Figs. 4(a) and (b) shows that the unmodulated representation adequately reveals the average structure, but of course, ignores the more subtle, local structure. These local density increases and decreases are readily apparent in certain regions of Fig. 4(b) as 'overlapping' adatoms and 'spaces' between adatoms, respectively. These density changes increase the adlayer elastic energy. However, the decrease in the adsorbate-substrate energy due to the modulation more than compensates for this increase. This is illustrated in Fig. 4(c), which shows the adatom shifts $\vec{u}_j$. The small filled (open) circles represent the adatoms positions in the modulated (unmodulated) adlayer; $\vec{u}_j$ is the difference between the two. This Figure shows a clear tendency for the adatoms to shift toward the lowest energy sites - the three-fold hollows. The shifts are largest midway between the low energy and high energy (on-top) sites, where the gradient of the adsorbate-substrate energy is large.

Our method of measuring the interference between the substrate scattering and the scattering caused by the spatial modulation of the incommensurate adlayer is more sen-

sitive to the modulation than measurements of the 'satellite' diffraction caused by the modulation. This is so because the interference depends on $(A_m)(A_s)$, which is linear in $\vec{u}_{\vec{G}}$, while the satellite intensity depends on $(A_m)^2$, which is quadratic in $\vec{u}_{\vec{G}}$ and much smaller. Thus, the satellite scattering has only been observed when the substrate induced modulation is strong and $\vec{u}_{\vec{G}}$ is large.[9] Indeed, in earlier measurements of UPD Pb on Ag(111), we could not observe any satellite diffraction peaks (e.g. the satellite intensity was less than 3% of the main Pb peak).[46] If $\vec{u}_{\vec{G}}(\vec{G} = (100)_h)$ for Pb on Ag(111) is similar to that for Tl on Ag(111), then the satellite peak intensity will be about 0.6% of the main peak, which explains why we were not able to observe it previously.[46] For Tl, this calculated peak intensity is only 100 counts per second (cps), which is small compared to the background scattering of about 2,000cps. In addition, by measuring the satellites, it is not possible to determine directly the relative phase of the scattering caused by the modulation, since $|\vec{G} \cdot \vec{u}_{\vec{G}}|^2$ is measured. In contrast, by measuring the interference between the adlayer and substrate scattering, this phase is readily determined.

It is interesting to compare our results with those of Reiter and Moss, who treated the x-ray scattering from a 2D *liquid* modulated by a periodic host substrate.[6] They found that the 2D liquid contributes scattering intensity to the substrate diffraction peaks, and from this contribution, the Fourier components of the surface energy corrugation $V_{\vec{G}}$ can be determined. Together with their co-workers, they have determined the Fourier components for Rb[7] and K[8] intercalated into graphite. For both a 2D liquid and a 2D solid, the origin of the contribution to the substrate scattering is the same, since it is the periodic spatial modulation induced by the substrate potential. Despite this, the contribution to the substrate scattering in these two situations is quite different, because the 'elastic' response of a solid to the substrate potential is very different from that of a liquid. A solid will support shear but a liquid will not. Thus, the solid's elastic response is determined by its phonon spectrum (e.g. sound velocities), while for a liquid the response is determined by temperature and the liquid's structure factor.[6] Although the origin of the substrate scattering contribution is the same for 2D

liquids and solids, the scattering amplitudes depend on quite different physical properties.

VI. Summary and Conclusions

By conducting in-situ measurements of the intensities of crystal truncation rods from Ag(111) substrates both with and without a monolayer of electrochemically adsorbed Tl, we have determined the longitudinal component of the first Fourier coefficient of the substrate-induced modulation of the incommensurate Tl monolayer (0.03Å). The observed changes in the x-ray scattering arise because the spatial modulation induced by the substrate potential has wavevectors commensurate with the substrate periodicity. Since the scans were made along the truncation rods, the spacing of the Tl monolayer above the Ag surface was also determined (3.05Å). The first Fourier component of the surface potential energy corrugation (2-3meV = 0.05-0.07kcal/mole) was estimated using the NM model[3, 4] and estimates of the elastic response of the Tl monolayer. Because the phase of the monolayer scattering amplitude (relative to the substrate) could be deduced, the sign of this Fourier component of the surface energy corrugation was determined. This identified the three-fold hollow sites as the lowest energy sites on the surface. The data were analyzed by taking the ratio of the truncation rod intensities with and without the monolayer adsorbed. This was very important, since the ratio is considerably more accurate than the intensities. The truncation rod scans of the bare surface show that the immersed Ag surface is very smooth (rms roughness of 0.7Å).

These results demonstrate for the first time that surface x-ray scattering measurements of the *substrate* diffraction can easily be used to probe the substrate-induced modulation of incommensurate adlayers. Similar measurements will provide important structural information on many other systems, such as the substrate-induced modulation in thin epitaxial layers, other incommensurate adlayers, and the top layers of some single crystals, such as Au(111) and Au(100).[47]

Acknowledgements

References

[1] F.C. Frank and J.H. van der Merwe, Proc. Roy. Soc. (London) A **198**, 205, 216 (1949).

[2] F.C. Frank and J.H. van der Merwe, Proc. Roy. Soc. (London) A **200**, 125, 261 (1949).

[3] A.D. Novaco and J.P. McTague, Phys. Rev. Lett. **38**, 1286 (1977).

[4] J.P. McTague and A.D. Novaco, Phys. Rev. B **19**, 5299 (1979).

[5] R.J. Birgeneau and P.M. Horn, Science **232**, 329 (1986).

[6] G. Reiter and S.C. Moss, Phys. Rev. B **33**, 7209 (1986).

[7] S.C. Moss, G. Reiter, J.L. Robertson, C. Thompson, J.D. Fan, and K. Ohshima, Phys. Rev. Lett. **57**, 3191 (1986).

[8] X.B. Kan, J.L. Robertson, S.C. Moss, K. Ohshima, and C.J. Sparks, Phys. Rev. B **39**, 10627 (1989).

[9] P.W. Stephens, P.A. Heiney, R.J. Birgeneau, P.M. Horn, D.E. Moncton, and G.S. Brown, Phys. Rev. B **29**, 3512 (1984).

[10] J. Villain and M.B. Gordon, Surf. Sci. **125**, 1 (1983).

[11] J.M. Cowley, J.B. Cohen, M.B. Salamon, and B.J. Wuensch, in *Modulated Structures-1979, Kailua Kona, Hawaii*, (American Institute of Physics, New York, 1979).

[12] R. Pynn, Nature **281**, 433 (1979).

[13] P. Bak, Rep. Prog. Phys. **45**, 587 (1982), (and references therein.).

[14] I.K. Robinson, Phys. Rev. B **33**, 3830 (1986).

[15] A.M. Afanas'ev, P.A. Aleksandrov, S.S. Fanchenko, V.A. Chaplanov, and S.S. Yakimov, Acta Cryst. **A42**, 116 (1986).

[16] S.R. Andrews and R.A. Cowley, J. Phys. C **18**, 6427 (1985).

[17] I.K. Robinson, W.K. Waskiewicz, R.T. Tung, and J. Bohr, Phys. Rev. Lett. **57**, 2714 (1986).

[18] R. Feidenhans'l, Surf. Sci. Reports **10**, 105 (1989).

[19] (This assumes that the substrate is rigid. Our analysis indicates this is valid, since there is no change in the substrate roughness on adsorption of the Tl.).

[20] S.G.J. Mochrie, Phys. Rev. Lett. **59**, 304 (1987).

[21] M.G. Samant, M.F. Toney, G.L. Borges, L. Blum, and O.R. Melroy, Surf. Sci. **193**, L29 (1988).

[22] M.G. Samant, M.F. Toney, G.L. Borges, L. Blum, and O.R. Melroy, J. Phys. Chem. **92**, 220 (1988).

[23] E.D. Specht, A. Mak, C. Peters, M. Sutton, R.J. Birgeneau, K.L. D'Amico, D.E. Moncton, S.E. Nagler, and P.M. Horn, Z. Phys. B **69**, 347 (1987).

[24] W.R. Busing and H.A. Levy, Acta Cryst. **22**, 457 (1967).

[25] D. Kolb, M. Przasnyski, and H. Gerischer, J. Electroanal. Chem. **54**, 25 (1974).

[26] D.M. Kolb, in *Advances in Electrochemistry and Electrochemical Engineering*, edited by H. Gerischer and C.W. Tobias, (Wiley, New York, 1978), Vol. 11, p. 125.

[27] D.M. Kolb, J. Vac. Sci. Technol. A **4**, 1294 (1986).

[28] H. Siegenthaler, K. Juttner, E. Schmidt, and W.J. Lorenz, Electrochim. Acta **23**, 1009 (1978).

[29] K. Juttner and H. Siegenthaler, Electrochim. Acta **23**, 971 (1978).

[30] W.J. Lorenz, H.D. Hermann, N. Wuthrich, and F. Hilbert, J. Electrochem. Soc. **121**, 1167 (1974).

[31] A. Bewick and B. Thomas, J. Electroanal. Chem. **65**, 911 (1975).

[32] M.F. Toney, J.G. Gordon, L.S. Kau, G. Borges, O.R. Melroy, M.G. Samant, D.G. Wiesler, D. Yee, and L.B. Sorensen, unpublished, 1990

[33] M.S. Altman, P.J. Estrup, and I.K. Robinson, Phys. Rev. B **38**, 5211 (1988).

[34] I.K. Robinson, Aust. J. Phys. **41**, 359 (1988).

[35] (Although stacking faults can give rise to scattering intensity similar to that from CTRs, we cannot fit the data shown in Figure 3 by assuming the film has stacking faults.).

[36] J.M. MacLaren, J.B. Pendry, R.J. Rous, D.K. Saldin, G.A. Somorjai, M.A. Van Hove, and D.D. Vvedensky, in *Surface Crystallographic Information Service: A Handbook of Surface Science*, (Reidel, Dordrecht, 1987).

[37] M.F. Toney and O.R. Melroy, in *Synchrotron Radiation in Materials Research, MRS Symp. Proc., Vol. 143*, edited by R. Clarke, (Materials Research Society, 1989), p. 375.

[38] M.F. Toney and O.R. Melroy, in *In-Situ Studies of Electrochemical Interfaces*, edited by H.D. Abruna, (VCH Verlag Chemical, 1990).

[39] K. Kern, P. Zeppenfeld, R. David, R.L. Palmer, and G. Comsa, Phys. Rev. Lett. 57, 3187 (1986).

[40] W.A. Steele, *The Interaction of Gasses with Solid Surfaces*, (Pergamon Press, Oxford, 1974).

[41] L.D. Landau and E.M. Lishitz, *Statistical Physics*, (Addison-Wesely, Reading, 1969).

[42] J.F. Nye, *Physical Properties of Crystals*, (Oxford University Press, London, 1957).

[43] G. Simmons and H. Wang, *Single Crystal Elastic Constants and Calculated Aggregate Properties: A Handbook*, (MIT Press, Cambridge, 1971).

[44] A.G. Naumovets and Yu.S. Vedula, Surf. Sci. Reports 4, 365 (1984).

[45] K.J. Rawlings, M.J. Gibson, and P.J. Dobson, J. Phys. D 11, 2059 (1978).

[46] O.R. Melroy, M.F. Toney, G.L. Borges, M.G. Samant, J.B. Kortright, P.N. Ross, and L. Blum, Phys. Rev. B 38, 10962 (1988).

[47] D. Gibbs, B.M. Ocko, D. M. Zehner, and S.G.J. Mochrie, Phys. Rev. B 38, 7303 (1988).

References

Figure Captions

Figure 1. One dimensional, schematic illustration of the spatial modulation induced by the substrate potential. (a) Unmodulated adlayer in the absence of a substrate. The adatom positions are $\vec{R}_j$. (b) Modulated adlayer. The adatom positions have shifted to $\vec{R}_j + \vec{u}_j$ due to the substrate potential. The spacing between atoms in the adlayer and substrate are a and b, respectively.

Figure 2. Cyclic voltammogram (current-voltage curve) for the deposition of Tl on Ag(111) in 2.5×10^{-3} M Tl_2SO_4 and 0.1M Na_2SO_4. The potentials were measured relative to Ag/AgCl and the scan rate was 2 mV/s. The first large peak (at approximately -470mV) corresponds to the deposition of a single monolayer of Tl, while the second peak corresponds to the deposition of a second layer (bilayer). The Nernst potential for bulk deposition is -710mV. The insert shows the adsorption isotherm, which is the integral of the cyclic voltammogram. There is a background current due to processes that do not involve deposition of Tl. A linear current (passing through the cyclic voltammogram at V = -600 and -180mV) was used to estimate this background current and has been subtracted from the data.

Figure 3. Intensity of the Ag $(10Q_z)_h$ crystal truncation rod. (a) Bare Ag surface at V = -200mV. The data are shown by the filled circles and the best fit by the solid line. (b) Tl monolayer on Ag at V = -600mV. The data are shown by the open circles and the best fit by the solid line. (c) The ratio of CTR intensity with the Tl monolayer present (b) to the CTR intensity with the monolayer absent (a). The data sets shown in (a) and (b) are both averages of eight separate CTR scans; they have a reproducibility of about 1.5%.

Figure 4. Schematic representation of one domain of monolayer Tl on Ag(111). The rotation angle between the Ag and Tl lattices is $\Omega = 4.5°$ and the average near-neighbor spacing of the Tl monolayer is 3.34Å.[32] The open circles represent atoms in the Ag(111) surface. (a) Unmodulated monolayer. (b) Modulated monolayer. The adatoms positions are calculated using Equation (1). The shaded circles represent the Tl atoms and the lower leftmost adatom is arbitrarily positioned above an Ag atom. (c) A comparison between the modulated and unmodulated monolayers. The small filled (open) circles represent the adatoms positions in the modulated (unmodulated) adlayer. The adatom shift $\vec{u}_j$ is the difference between the two.
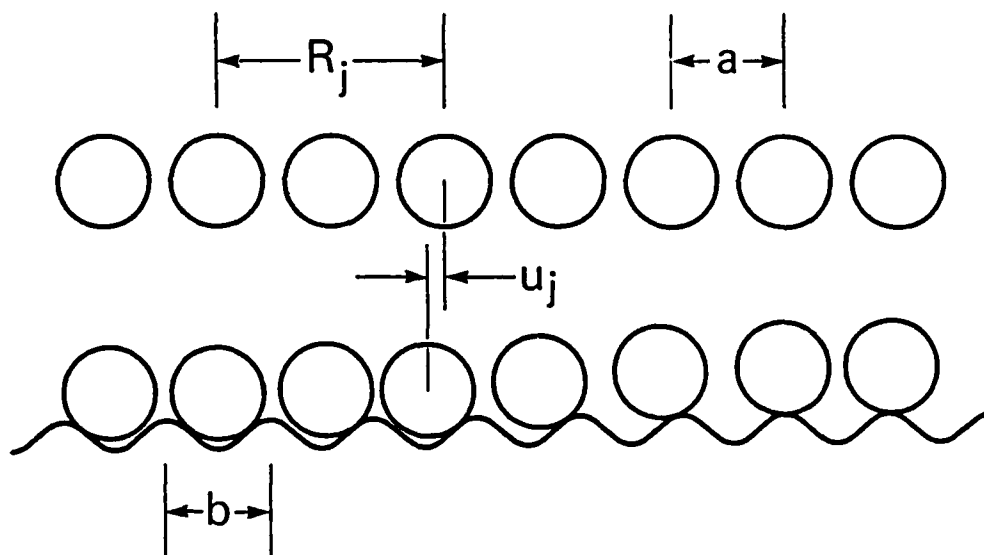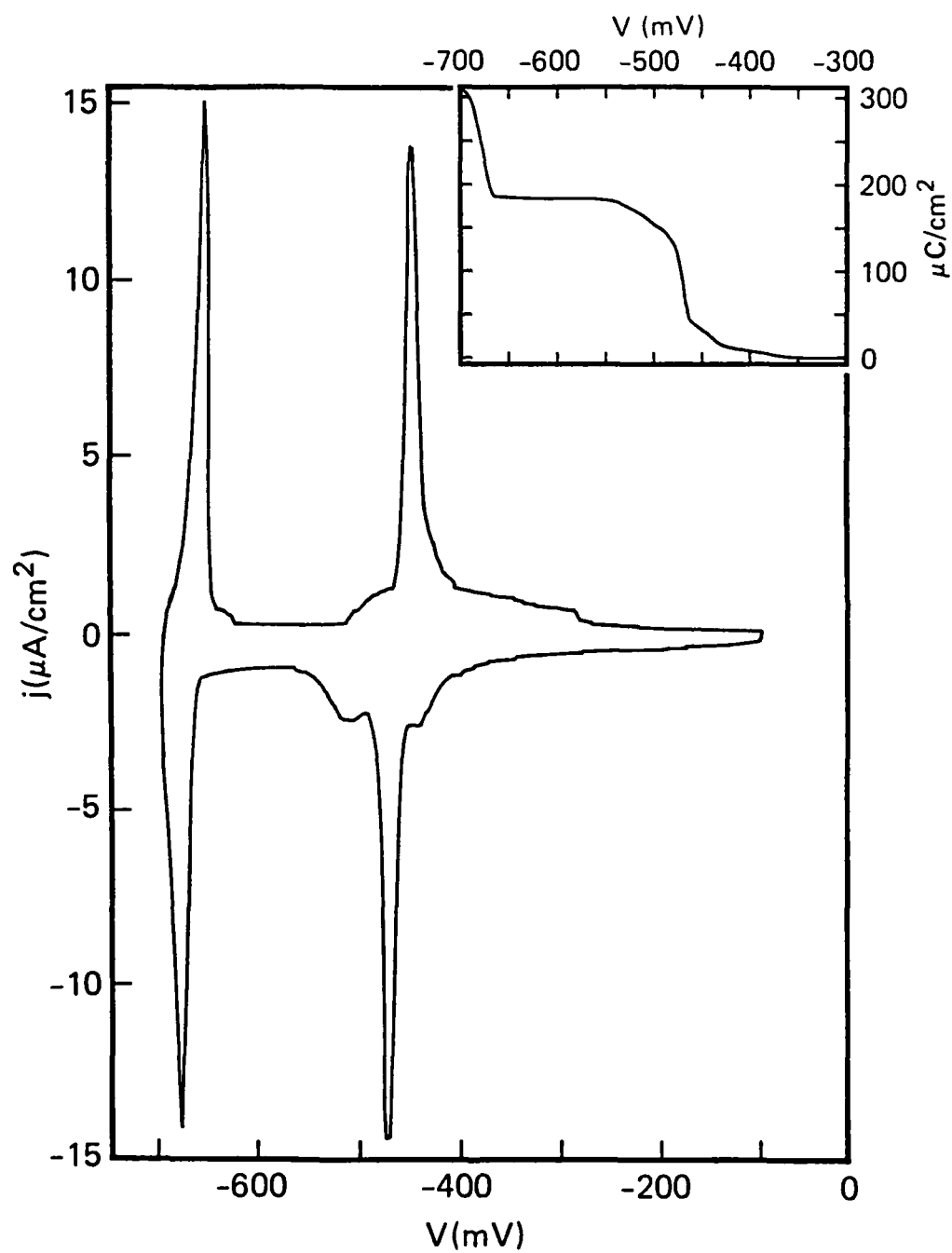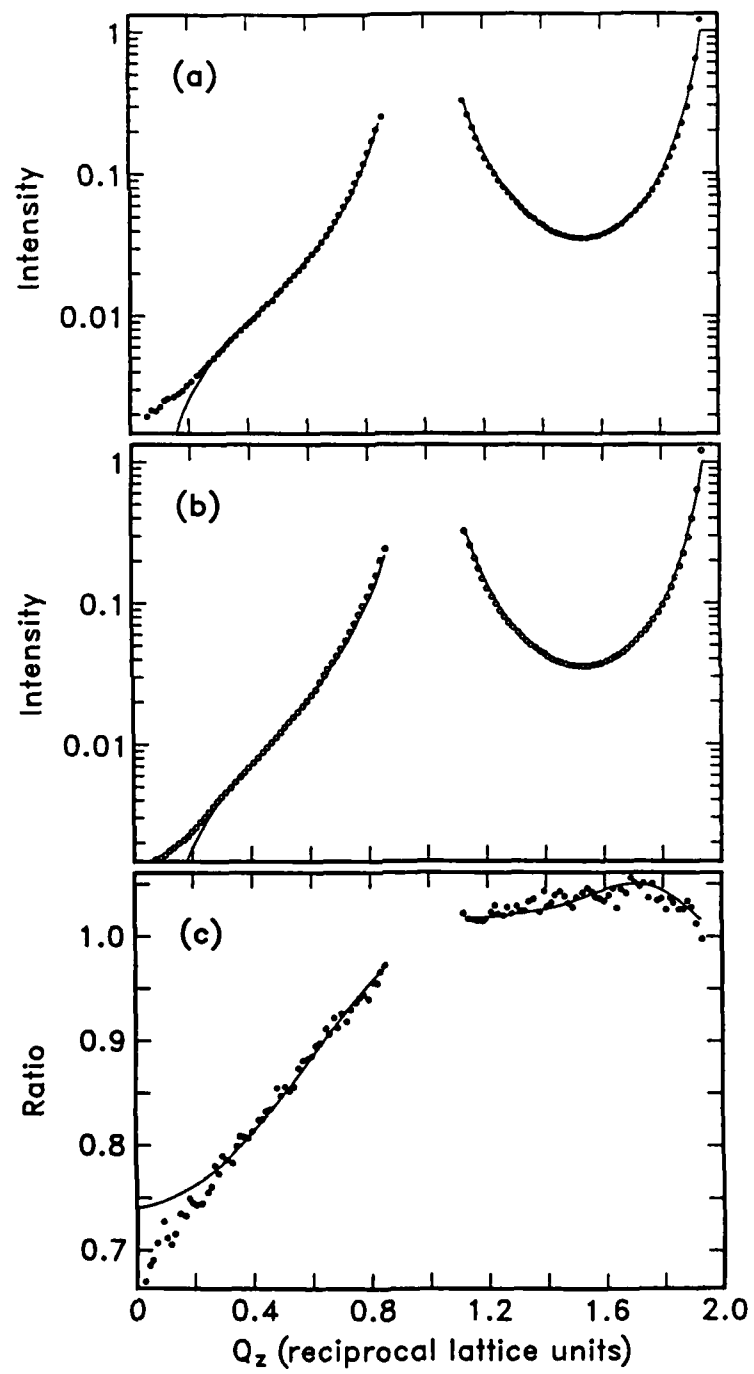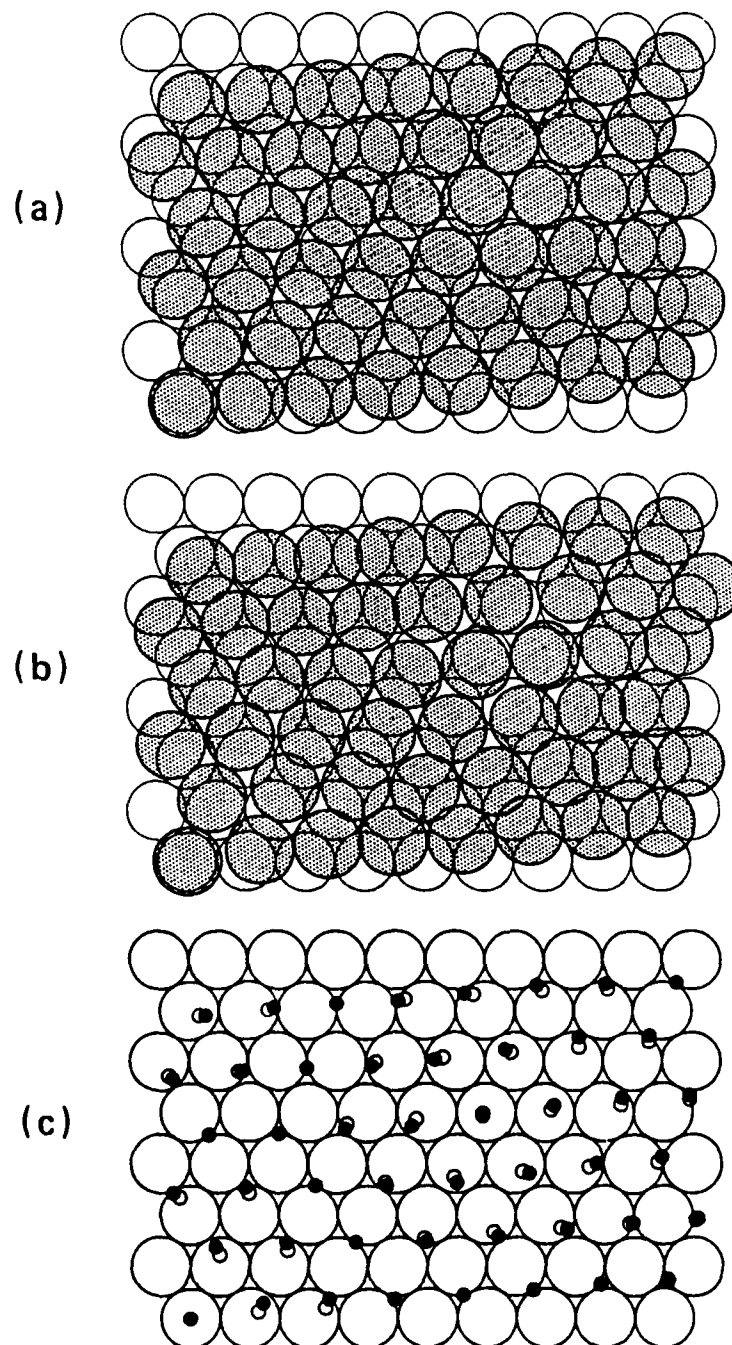
Figure 1

Figure 2

Figure 3

(a)

(b)

(c)

Figure 4